

Aviation Impact on Air Quality Present Day and Mid-Century Simulated in the Community Atmosphere Model (CAM)

Authors: Daniel Phoenix¹, Arezoo Khodayari², Donald Wuebbles³ and Kevin Stewart²

¹ University of Oklahoma, OK, USA

² California State University Los Angeles, CA, USA

³ University of Illinois, Urbana, IL, USA

Correspondence to: Arezoo Khodayari (akhoday@calstatela.edu)

Abstract

The projected increase in global air traffic raises concerns about the potential impact aviation emissions have on climate and air quality. Previous studies have shown that aircraft non-landing and take-off (non-LTO) emissions (emitted above 1 km) can affect surface air quality by increasing concentrations of ozone (O₃) and fine particles (PM_{2.5}). Here, we examine the global impacts of aviation non-LTO emissions on surface air quality for present day and mid-century (2050) using the Community Atmosphere Model with Chemistry, version 5 (CAM5). An important update in CAM5 over previous versions is the modal aerosol module (MAM), which provides a more accurate aerosol representation. Additionally we evaluate of the aviation impact at mid-century with two fuel scenarios, a fossil fuel (SC1) and a biofuel (Alt). Monthly-mean results from the present day simulations show a northern hemisphere (NH) mean surface O₃ increase of 1.3 ppb (2.7% of the background) and a NH maximum surface PM_{2.5} increase of 1.4 µg/m³ in January. Mid-century simulations show slightly greater surface O₃ increases (mean of 1.9 ppb (4.2%) for both scenarios) and greater PM_{2.5} increases (maximum of 3.5 µg/m³ for SC1 and 2.2 µg/m³ for Alt). While these perturbations do not significantly increase the frequency of extreme air quality events (increase is less than 1.5%), they do

contribute to the background concentrations of O₃ and PM_{2.5}, making it easier for urban areas to surpass these standards.

1. Introduction

Aviation emits gases and particles that are a concern for air quality and human health. Aviation emits nitrogen oxides (NO_x = NO + NO₂), volatile organic compounds (VOCs), sulfur oxides (SO_x), soot, and other particles, which have an impact on the concentrations of ozone, and fine particles at the surface (Brasseur et al., 1996; IPCC, 1999; Lee et al., 2010, Cameron et al., 2017). Additionally, between 1989 and 2009, aviation has grown at a rate of 4.4% per year and has generally outpaced economic growth (ICAO, 2010). Given the potential impacts that aviation may have on air quality and human health, and the rapid growth of the aviation sector, it is important to assess the current and future impact that aviation may have. Recently a study by Cameron et al. (2017) used five global atmospheric computer models to evaluate the effects of global aircraft emissions on surface air quality by calculating changes in ozone and small particles. This study evaluated the global air quality effects due to all aviation emissions (i.e. both LTO and cruise emissions) and reported a near-surface annual changes in ozone of 0.3 to 1.9%, and near-surface annual changes in PM_{2.5} of -1.9 to 1.2%, globally.

Most earlier studies only considered the effects of landing and take-off emissions (LTO) on air quality (Herndon et al., 2004; Schurmann et al., 2007; Herndon et al., 2008). While aviation does have a localized effect on air quality near airports due to landing and take-off emissions, recent modeling studies suggest that aviation non-LTO emissions (i.e. cruise altitude emissions), emitted in the upper troposphere and lower

stratosphere (UTLS), do have an impact on surface air quality by increasing the concentrations of O₃ and particulate matter of 2.5 microns and smaller (PM_{2.5}) at the surface (Barrett et al., 2010a; Jacobson et al., 2013; Lee et al., 2013).

Barrett et al. (2010a) first examined the impacts of aviation cruise emissions on surface air quality and put them in terms of human mortality. Using the Goddard Earth Observing System model with Chemistry (GEOS-Chem), a three dimensional chemical transport model (CTM), the study suggested that aviation cruise emissions, while contributing ~ 1% of air quality related mortalities, comprises 80% of aviation emission deaths. The study found that secondary H₂SO₄ – HNO₃ – NH₃ aerosols are mainly responsible for premature mortalities and that aviation cruise emissions are responsible for ~ 8000 premature mortalities per year.

Lee et al. (2013) then used the Community Atmosphere Model version 3 (CAM3) CTM to evaluate the effect of aviation cruise emissions on surface air quality. That study found that aviation non-LTO emissions increased surface O₃ regionally by up 1-2 ppbv in January and ~0.5 ppbv in July and surface PM_{2.5} by ~0.5% (less than 0.2 µg/m³). Additionally, while most perturbations were not statistically significant, the statistically significant perturbations were less than 1% of the background. It is noted that background concentration of any pollutant within the context of this paper refers to atmospheric concentration of that pollutant in the absence of aviation emissions. A mortality estimate was not done for this study due to uncertainties with health impacts of such low PM_{2.5} increases.

In a similar study, Jacobson et al. (2013), using the Gas, Aerosol, Transport, Radiation, General-Circulation, Mesoscale, and Ocean Model (GATOR-GCMOM)

chemical response model (CRM), found that aviation cruise emissions increased surface ozone by ~0.4%. Additionally, surface PAN was increased by ~0.1%. It was estimated that ~620 deaths per year were attributed to aviation cruise emissions, with about half due to ozone and half due to PM_{2.5}.

To further examine the impact of aviation non-LTO emissions on surface air quality we used the latest version of CAM5 (Community Atmosphere Model version 5), the atmospheric component model for the Community Earth System Model (CESM). Moreover, we did examine the future impact of aviation non-landing and take-off (non-LTO) emissions on surface air quality for the year 2050 and for two different future scenarios.

A major update in CAM5 relative to its previous versions is the inclusion of a modal aerosol module (MAM), which provides a more accurate representation of aerosols. The use of modal aerosol model allows the prediction of aerosol mass and the total number in each mode as opposed to aerosol bulk model that prescribes a fixed size distribution for aerosols and this allow a more representative simulation of aerosols Surface Area Density (SAD). Aerosols surface area density has relevance for heterogeneous reactions occurring on the surface of aerosol particles since these reactions do not directly relate to the aerosol mass but rather depend on the amount of tropospheric SAD. SAD depends not only on aerosol mass but also on their size distribution. As such, the use of modal aerosol model in CAM5 helps to better simulate the reactions that have relevance for calculations of aviation-induced changes in aerosols.

This paper goes beyond the model intercomparison study by also providing the first evaluation of the mid-century (2050) impact of aviation non-LTO emissions on surface

air quality. The mid-century aviation impact was analyzed assuming two different jet fuels, a standard scenario assuming use of fossil fuels, and a scenario assuming the use of biofuels, with the assumption of 50% less soot and no sulfur emissions compared to the fossil fuel scenario.

The rest of this paper is organized as follows. Section 2 describes the model and simulation set up. Results of the present day and mid-century simulations are presented in section 3 and concluding remarks are presented in section 4.

2. Model Description and Simulation Set-up

Simulations were run with CAM5. The model includes tropospheric and stratospheric chemistry, with 133 species and 330 photochemical reactions described in Lamarque et al. (2012). A major update over previous versions of CAM is the modal aerosol module (MAM) for aerosol treatment (Liu et al., 2012).

MAM was developed with two versions, one with seven lognormal modes (MAM7) and one with three lognormal modes (MAM3) (Liu et al., 2012). For this study, MAM7 was used which represents Aitken, accumulation, primary carbon, fine dust and sea salt, and coarse dust and sea salt modes. Within each mode, aerosol mass mixing ratios and number mixing ratios are calculated (Liu et al., 2012). Within a single mode, MAM7 simulates mass mixing ratios for internally-mixed sulfate (SO_4), ammonium (NH_4), secondary organic aerosol (SOA), primary organic matter (POM) and black carbon (BC) aged from the primary carbon mode, sea salt, and the number mixing ratio of accumulation mode particles. POM and BC are first emitted to the primary carbon mode, then aged and transferred to the accumulation mode by condensation of H_2SO_4 ,

NH₃ and semi-volatile organics and by coagulation with Aitken and accumulation modes. The size distributions of each mode are assumed to be lognormal, with the mode dry or wet radius varying as number and total dry or wet volumes change. The geometric standard deviation of each mode is prescribed (Easter et al., 2004 and references therein), along with the typical size range of each mode. There are 31 total transported aerosol tracers. MAM simulates both internal and external mixing of aerosols, chemical and optical properties of aerosols, and various complicated aerosols processes (Liu et al., 2012). The transported gas species are sulfur dioxide (SO₂), hydrogen peroxide (H₂O₂), dimethyl sulfide (DMS), sulfuric acid gas vapor (H₂SO₄), ammonia (NH₃), and a lumped semi-volatile organic species.

Non-aircraft anthropogenic emissions are taken from the IPCC AR5 emission inventory, assuming the RCP 4.5 background emissions trajectory (Clarke et al., 2007). The background emissions of non-aviation short-lived species (e.g., NO_x, VOCs) are taken from the IPCC RCP4.5 scenario (van Vuuren et al., 2011) while longer-lived species (e.g., carbon dioxide (CO₂), methane (CH₄), chlorofluorocarbons (CFCs), and nitrous oxide (N₂O)) were specified as boundary conditions based on the IPCC RCP4.5 scenario. Since the IPCC AR5 data set does not provide emissions of natural aerosols and precursor gases: volcanic sulfur, DMS, NH₃, and biogenic volatile organic compounds, AeroCom (AEROSol Comparisons between Observations and Models) emission fluxes, injection heights and size distributions for volcanic SO₂ and sulfate and the surface DMS flux are used. The emission flux of NH₃ is prescribed from the MOZART-4 data set (Emmons et al., 2010). The Model of Emissions of Gases and Aerosols from Nature (MEGAN) (Guenther et al., 2006) was used to obtain the background emissions of

biogenic species such as isoprene, monoterpenes, toluene, big alkenes, and big alkanes (which are used to derive emissions of the semi-volatile organic species). For the present day simulations, the emissions described above are from the year 2005, while emissions for the mid-century simulations are from the year 2050.

CAM5 present day simulations were run with a horizontal resolution of 2° latitude x 2.5° longitude with 56 vertical levels from the surface up to ~ 2 hPa. To reduce the year-to-year climate variability in the model simulations and to better detect the aviation NO_x -induced signal, specified dynamics (“off-line” mode) simulations were performed. In the specified dynamics mode a fixed meteorology is used for all the simulation years to reduce year-to-year climate variability or eliminate meteorological noise. The model was driven with 2006 meteorology from MERRA (Modern Era Retrospective-Analysis for Research and Applications) reanalysis for seven years, with the final year used for analysis. MERRA meteorology fields exist on 56 vertical level, as such present day simulation were configured with 56 vertical levels. It is noted that running the model in the specified dynamics mode does not allow the feedback of aviation impacts or chemistry on the background meteorology or the radiation scheme and as such results presented here are obtained in absence of such feedback.

The CAM5 mid-century simulations also have a horizontal resolution of 2° latitude x 2.5° longitude but with 30 vertical layers, with the top layer at ~ 2 hPa. The meteorology field for 2050 specified dynamic simulations was obtained by running CAM5 for five model years in a coupled mode (i. e. with interactive chemistry and meteorology). The meteorology fields from the fifth year were extracted to drive the mid-century simulations. Since CAM5 in the coupled mode runs on 30 vertical levels the

obtained meteorology fields were also on 30 levels and as such mid-century simulations were configured with 30 vertical levels. The mid-century simulations were then run for seven years in the specified dynamic model, with the final year used for analysis.

For the 2006 aviation emissions, CAM5 simulations use the AEDT gridded emissions inventory, described in Wilkerson et al. (2010). The mid-century simulations used two different fuel scenarios, a fossil fuel scenario and a biofuel scenario. These mid-century aviation emission scenarios are produced based on projected population growth by 2050, consider identical flight tracks and flight distance to the year 2006, and have certain assumptions about future fuel efficiency or fuel type (Barret et al., 2010b). The fossil fuel scenario, Scenario 1 (SC1), assumes continued fuel efficiency by 2050 based on technological improvements, maintaining a 2 %/yr improvement in aviation system efficiency and a NO_x-related technology improvement consistent with published ICAO/CAEP scenarios to 2036 extended to 2050 based on NASA N+3 and N+4 targets of “better than 75%”. The biofuel, or the Alternative Fuel scenario (Alt), has the same fuel burn as Scenario 1 but has no sulfur and 50% less BC (soot) emissions. To analyze the effect of aviation emissions on global air quality, two simulations are performed in each simulation set (i.e present day simulation set and the two mid-century simulation sets). One simulation considers all anthropogenic emissions including aviation emissions (perturbed run), and the other simulation has all anthropogenic emissions but no aviation emission (control run). The difference between these two simulations corresponds to the changes induced by aviation emissions. To examine the impact of non-LTO emissions, aviation emissions below 1 km were set to zero. The following list contains all the simulation sets:

1) Present day simulations: 2006 climate, 2006 perturbed run (all anthropogenic emissions including 2006 aviation non-LTO emissions), and a control run (all anthropogenic emissions but no aviation emissions).

2) Mid-century simulations: 2050 climate, 2050 perturbed run (all anthropogenic emissions including 2050 aviation non-LTO emissions from SC1 scenario), and a control run.

3) Mid-century simulations: 2050 climate, 2050 perturbed run (all anthropogenic emissions including 2050 aviation non-LTO emissions from Alt scenario), and a control run.

Table 1 compares the non-LTO present day fuel emissions to the two mid-century fuel scenarios.

3. Results and Discussion

3.1 Effects on NO_x and O₃

Aviation NO_x emissions increase the concentrations of O₃ in the UTLS. As O₃ is transported towards the surface, it converts surface NO_x to HNO₃. Figure 1 shows the surface NO_x difference between the simulations with and without aviation emissions for January and July. For the mid-century simulations, only Scenario 1 is shown for NO_x and O₃ (Figure 2, below) because the aviation emissions that affect NO_x and O₃ concentrations at the surface are the same between the two mid-century fuel scenarios. As shown in Figure 1, aviation emissions consume NO_x at the surface in January more than in July. In January, more O₃ is transported to the surface than in July, which converts more NO_x to HNO₃. Similarly, in mid-century, the NO_x perturbation is more negative in January. Compared to present day, the absolute difference is lower in the mid-century

simulations, however, the background NO_x concentration is much lower in the mid-century simulations, such that the relative difference (compared to the background), is much higher in mid-century. Aviation emissions decrease the mean NH January NO_x concentration at the surface by 62% and 86% of the background in present day and mid-century, respectively.

The surface running 8-hour mean O₃ perturbation, averaged over a month, is shown in Figure 2. Running 8-hour averages are computed from the hourly ozone concentration data and are computed over successive 8-hour blocks. As expected, the largest O₃ perturbations are in the northern hemisphere, where the majority of aviation emissions occur. Consistent with previous studies, the impact is greater in January than July due to heterogeneous reactions (Lee et al., 2013). The mean surface O₃ NH perturbation is 1.3 ppb (2.7% of the background) and 0.4 ppb (1% of the background) in January and July, respectively. The mid-century SC1 mean NH perturbation is 1.6 ppb (3.7% of background) and 0.59 ppb (1.8% of the background) in January and July, respectively. The relative mid-century impact is slightly larger than the present day impact (for both months), however, it is still small relative to the background. Additionally, while the difference between the two mid-century fuel scenarios is small, it should be noted that the mean NH surface O₃ perturbation is slightly higher in the Alternative fuel scenario (not shown), with a mean NH perturbation of 1.8 ppb (4.1% of the background) and 0.65 ppb (2.0% of the background) in January and July, respectively. The difference in aviation-induced ozone between SC1 and Alternative fuel scenario is likely due to more photolysis and production of O₃ in the UTLS and less removal of NO₃ and N₂O₅ due to heterogeneous chemistry in the Alternative fuel

scenario, which has no sulfur. It is noted that higher sulfate concentrations likely results in higher reflection of incoming solar radiation and consequently less photolysis rate, and in higher surface area of sulfate aerosols and as such enhances those reactions that occur on the surface area of these aerosols such as removal of NO_3 and N_2O_5 due to heterogeneous chemistry.

Table 2 shows the maximum surface aviation-induced O_3 perturbations in January and July for several regions, the Eastern USA, Western USA, Europe, and Southeast Asia, for present day and mid-century, respectively. Despite the larger O_3 increases in January, the background O_3 concentrations are much lower in January than in July in the Northern Hemisphere. As shown in Table 2, aviation increases surface O_3 by up to 1-2 ppb regionally in January for present day. For July, aviation increases surface O_3 by about 0.5-1 ppb regionally in present day. These numbers are in good agreement with Lee et al. (2013). For present day, surface O_3 in January increases about 3-4% relative to the background from aviation emissions.

Mid-century simulations indicate that the aviation impact will be slightly larger for the same regions by 2050, increasing O_3 relative to background concentrations by 4-6% for most regions, and up to 10% for East Asia. However, the mean background O_3 concentrations in the four regions for both present day and mid-century are well below the EPA NAAQS standard for ozone (75 ppbv, averaged over 8-hours). It should also be noted that these regional air quality analyses are restricted to the $\sim 2^\circ \times 2.5^\circ$ model resolution.

3.2 Effects on aerosols

Just as O_3 is a concern for air quality and effects on human health, $PM_{2.5}$ poses important health implications as well by increasing the risk of respiratory and cardiovascular morbidity through aggravated asthma and lung cancer. Figure 3 shows the surface $PM_{2.5}$ aviation-induced perturbations for present day (top) and the two mid-century fuel scenarios (SC1-middle, Alt-bottom). Unlike O_3 , the surface $PM_{2.5}$ perturbations are not as homogeneously distributed due to the shorter lifetime of the aerosols. As shown in Figure 3, aviation emissions increase $PM_{2.5}$ at the surface in January more than July, consistent with Barrett et al. (2010a) and Lee et al. (2013). This is due to the surface NO_x being converted to HNO_3 from aviation-induced O_3 . The increased HNO_3 then determines the effects of aviation non-LTO emissions on the surface aerosols (Lee et al., 2013). Therefore, it is the aviation NO_x emissions, not the aerosol emissions that determine the $PM_{2.5}$ perturbation at the surface (Lee et al., 2013). However, it is likely that changes in aerosol emissions at cruise altitudes could cause indirect changes in the $PM_{2.5}$ perturbation at the surface through changes in cloudiness and consequent perturbation of photolysis rates, and the production of aviation-induced ozone.

Aviation increases present day surface $PM_{2.5}$ concentrations by up to $1.4 \mu g/m^3$ in China in January. The maximum impact in mid-century is also in January for both fuel scenarios, with a maximum increase of $3.5 \mu g/m^3$ for SC1 in Africa and $2.2 \mu g/m^3$ for Alt in China. The maximum $PM_{2.5}$ increases in the continental U.S. and Europe are smaller ($\sim 0.1 \mu g/m^3$ in USA and $< 0.5 \mu g/m^3$ in Europe) for present day and mid-century. These regional perturbations agree with Lee et al. (2013), however they are not as spatially distributed as in Barrett et al. (2010a) and Lee et al. (2013).

Aviation increases $PM_{2.5}$ mainly by increasing surface sulfate (SO_4^{2-}) and ammonium nitrate (NH_4NO_3). Figures 4 and 5 show the surface SO_4^{2-} and NH_4NO_3 perturbations, respectively. OC and BC perturbations are relatively small, consistent with Barrett et al. (2010a) and Lee et al (2013).

As shown in Figs. 4 and 5, the SO_4^{2-} aviation-induced perturbation is much larger than the NH_4NO_3 perturbations for both January and July and for present day and mid-century scenarios. Thus, contrary to previous studies, NH_4NO_3 does not dominate the $PM_{2.5}$ perturbation in the boundary layer in January (Barrett et al., 2010a; Lee et al., 2013). In the present day simulations, for example, the peak NH_4NO_3 perturbation in January is $0.33 \mu g/m^3$ in East Asia. However, the peak SO_4^{2-} perturbation in East Asia is larger ($0.95 \mu g/m^3$). A possible explanation for these differences is that the previous studies used a bulk representation of aerosols in their models. CAM5 uses a modal aerosol module and does not assume ammonia is in equilibrium between the gas and aerosol phase which could explain the lower NH_4NO_3 perturbation in January in these simulations. It is further noted that considering the high uncertainty in NH_3 emissions sources and its critical role in the formation of NH_4NO_3 the aerosol changes resulting from aviation emissions remains to be highly uncertain.

3.3 Impact on extreme air quality events

To assess the aviation impact on the frequency of extreme air quality events, the frequency of exceedances of the EPA NAAQS standard due to aviation emissions for O_3 and $PM_{2.5}$ was assessed. Three regions were examined, representing the USA, Europe and East Asia. Tables 3 and 4 summarize the results for O_3 and $PM_{2.5}$, respectively. For O_3 , July is shown because even though the aviation effect is greatest in January, the

background O₃ concentrations are much higher in July. Therefore, aviation emissions may more readily contribute to extreme air quality events for O₃. For PM_{2.5}, January is shown since the aviation effect is larger in January. Additionally, for mid-century, only SC1 was shown, since there was little difference between the results of the two fuel scenarios. As shown in the tables, for both O₃ and PM_{2.5} and for present day and mid-century, aviation has a small impact on increasing the frequency of extreme air quality events. As shown in Table 3, the maximum impact for O₃ events is in Europe in mid-century, with a maximum increase less than 1.5%. For PM_{2.5} (Table 4), the impact is very low (~0.1%). It should be noted that such a small contribution from aviation to increase the frequency of extreme air quality events is partially due to the fact that background concentration of O₃ and PM_{2.5} when averaged over the model resolution are mostly below the EPA NAAQS, and partially due to the fact that our regional air quality analyses is restricted to the ~2° x 2.5° model resolution.

While previous studies have suggested that aviation does have an impact on air quality and health effects by increasing concentrations of O₃ and PM_{2.5} at the surface, these simulations suggest that, especially for PM_{2.5}, the aviation impact is very low. Differences between this study and prior studies may be due to differences in the treatment of aerosols in the models used. The bulk treatment, as used in previous studies, may have lead to an overestimation of PM_{2.5} by giving larger concentrations of NH₄NO₃ in the boundary layer in January, which was not seen in these simulations that used a modal aerosol module. Additionally, models that had a bulk treatment showed more disperse PM_{2.5} aviation-induced perturbations than this study, which also may have contributed to a large estimate of human mortalities.

4. Conclusions

The present day and mid-century global impact of aviation non-LTO emissions on surface air quality were evaluated with CAM5. The mid-century (2050) simulations had two fuel scenarios, a fossil fuel (SC1) which assumed some technological advancement, and a biofuel (Alt), which differed from the fossil fuel in that it had 50% less soot and no sulfur emissions. Aviation emissions increase surface O₃ concentrations mainly in the NH. The impact is larger in January, when the background O₃ concentrations are lower, compared to July. The overall NH aviation impact on O₃ is larger in mid-century compared to present day (up to ~4% and 2.7% of the background in mid-century and present day, respectively). Biofuels have little difference on surface O₃ concentrations compared to fossil fuels. Aviation increases PM_{2.5} concentrations by up to 1.4 µg/m³ in present day and mid-century PM_{2.5} concentrations by up to 3.5 µg/m³ and 2.2 µg/m³ in SC1 and Alt, respectively. Additionally, according to the data presented in Table 3 and 4 aviation has a very small impact on increasing the frequency of O₃ extreme air quality events and has essentially no impact on the frequency of PM_{2.5} extreme air quality events. Compared to previous studies, our surface O₃ and PM_{2.5} aviation-induced perturbations are about the same or lower, especially for PM_{2.5}, which is not a spatially dispersed as in Barrett et al. (2010a), Jacobson et al. (2013) and Lee et al. (2013). Given that mortality numbers should be correlated with the air quality standard violations incidents our results suggest that previous studies, which attributed high mortality rates to aviation non-LTO emissions, may have overestimated the impact on premature deaths. However, it is important to keep in mind that this study was an evaluation of the global, large scale

impacts of aviation on surface air quality. Full resolution of urban scale air quality events could not be resolved due to the model resolution used in this study ($\sim 2^\circ \times 2.5^\circ$). Due to the coarse model resolution the results obtained in this study are merely representative of large scale air quality effects and it is likely that the peak concentrations in populated areas have been underestimated.

Acknowledgements

The authors would like to thank the Federal Aviation Administration, Aviation Climate Change Research Initiative (ACCRI) for support under Contract #: 10-C-NE-UI amendment 001 and The Partnership for AiR Transportation Noise and Emissions Reduction (PARTNER). The opinions, findings, and conclusions or recommendations expressed in this material are those of the authors and do not necessarily reflect the views of ACCRI, PARTNER, or the FAA. We would like to acknowledge high-performance computing support from Yellowstone (ark:/85065/d7wd3xhc) provided by NCAR's Computational and Information Systems Laboratory, sponsored by the National Science Foundation.

References

- Barrett, S. R. H., R. E. Britter, and I. A. Waitz (2010a), Global mortality attributable to aircraft cruise emissions, *Environ. Sci. Technol.*, *44*, 7736-7742.
- Barret, S., Prather, M., Penner, J., Selkirk, H., Balasubramania, S., Doppelheuer, A., Fleming, G., Gupta, M., Halthore, R., Hileman, J., Jacobson, M., Kuhn, S., Lukachko, S., Miake-Lye, R., Petzold, A., Roof, C., Schaefer, M., Schumann, U., Waitz, I., and Wayson, R. (2010b), Guidance 25 on the Use of AEDT

Gridded aircraft Emissions in Atmospheric Models, version 2.0, Tech. rep.,
Federal Aviation Administration.

Brasseur, G. P., Muller, J. F., and Granier, C. (1996), Atmospheric impact of NO_x
emissions by subsonic aircraft: A three-dimensional model study, *J. Geophys.*
Res.-Atmos., 101, 1423–1428, 1996.

Cameron, M. A., Jacobson, M. Z., Barrett, S. R. H., Bian, H., Chen, C. C., Eastham, S.
D., (2017), An intercomparative study of the effects of aircraft emissions on
surface air quality. *Journal of Geophysical Research: Atmospheres*, 122, 8325–
8344. <https://doi.org/10.1002/2016JD025594>.

Clarke, L., J. Edmonds, H. Jacoby, H. Pitcher, J. Reilly, R. Richels (2007), Scenarios of
Greenhouse Gas Emissions and Atmospheric Concentrations. Sub-report 2.1A of
Synthesis and Assessment Product 2.1 by the U.S. Climate Change Science
Program and the Subcommittee on Global Change Research. Department of
Energy, Office of Biological & Environmental Research, Washington, 7 DC.,
USA, 154 pp,
<http://tntcat.iiasa.ac.at:8787/RcpDb/dsd?Action=htmlpage&page=compare>,
Accessed February 4, 2014.

Easter, R. C., S. J. Ghan, Y. Zhang, R. D. Saylor, E. G. Chapman, N. S. Laulainen, H.
Abdul-Razzak, L. R. Leung, X. Bian, and R. A. Zaveri (2004), MIRAGE: Model
description and evaluation of aerosols and trace gases, *J. Geophys. Res.*, 109.

Emmons, L. K. et al. (2010), Description and evaluation of the Model for Ozone and
Related chemical Tracers, version 4 (MOZART-4), *Geosci. Model Dev.*, 3, 43–67.

Guenther, A., T. Karl, P. Harley, C. Wiedinmyer, P. I. Palmer, and C. Geron (2006),
Estimates of global terrestrial isoprene emissions using MEGAN (Model of
Emissions of Gases and Aerosols from Nature), *Atmos. Chem. Phys.*, 6, 3181–
3210.

Herndon, S. C., Shorter, J. H., Zahniser, M. S., Nelson, D. D., Jayne, J., Brown, R. C.,
Miake-Lye, R. C., Waitz, I., Silva, P., Lanni, T., Demerjian, K., and Kolb, C.
E. (2004), NO and NO₂ emission ratios measured from in-use commercial aircraft
during taxi and takeoff, *Environ. Sci. Technol.*, 38, 6078–6084,
[doi:10.1021/Es049701c](https://doi.org/10.1021/Es049701c).

Herndon, S. C., Jayne, J. T., Lobo, P., Onasch, T. B., Fleming, G., Hagen, D. E.,
Whitefield, P. D., and Miake-Lye, R. C. (2008), Commercial aircraft engine
emissions characterization of in-use aircraft at Hartsfield-Jackson Atlanta
International Airport, *Environ. Sci. Technol.*, 42, 1877–1883,
[doi:10.1021/Es072029](https://doi.org/10.1021/Es072029).

- International Civil Aviation Organization (ICAO), 2010. ICAO Environmental Report 2010. Aviation and Climate Change. Available from: <http://www.icao.int/icao/en/env2010/Pubs/EnvReport10.htm> (accessed on 21 July 2011).
- Jacobson, M. Z., J. T. Wilkerson, A. D. Naiman, and S. K. Lele (2013), The effects of aircraft on climate and pollution. Part II: 20-year impacts of exhaust from all commercial aircraft worldwide treated individually at the subgrid scale, *Faraday Discuss.*, *165*, 369-382.
- Lamarque, J.-F., L. K. Emmons, P. G. Hess, D. E. Kinnison, S. Tilmes, F. Vitt, C. L. Heald, E. A. Holland, P. H. Lauritzen, and J. Neu (2012), CAM-chem: Description and evaluation of interactive atmospheric chemistry in the Community Earth System Model, *Geosci. Model Dev.*, *5*, 369-411.
- Lee D.S., D. Pitari, V. Grewe, K. Gierens, J.E. Penner, A. Petzold, M.J. Prather, U. Schumann, A. Bais, T. Berntsen, D. Iachetti, L.L. Lim, R. Sausen. Transport impacts on atmosphere and climate: aviation. *Atmospheric Environment*, *44* (2010), pp. 4678–4734. <http://dx.doi.org/10.1016/j.atmosenv.2009.06.005>
- Lee, H., S. C. Olsen, D. J. Wuebbles, and D. Youn (2013), Impacts of aircraft emissions on the air quality near the ground, *Atmos. Chem. Phys.*, *13*, 5505-5522.
- Liu, X. et al. (2012), Toward a minimal representation of aerosols in climate models: description and evaluation in the Community Atmosphere Model CAM5, *Geosci. Model Dev.*, *5*, 709-739.
- Penner, J. E., (1999) Aviation and the global atmosphere : a special report of IPCC Working Groups I and III in collaboration with the Scientific Assessment Panel to the Montreal Protocol on Substances that Deplete the Ozone Layer, Cambridge University Press, Cambridge.
- Schurmann, G., Schafer, K., Jahn, C., Hoffmann, H., Bauerfeind, M., Fleuti, E., and Rappengluck, B., (2007), The impact of NO_x, CO and VOC emissions on the air quality of Zurich airport, *Atmos Environ*, *41*, 103–118, doi:10.1016/j.atmosenv.2006.07.030, 2007.
- Whitt, D. B., M. Z. Jacobson, J. T. Wilkerson, A. D. Naiman, and S. K. Lele (2011), Vertical mixing of commercial aviation emissions from cruise altitude to the surface, *J. Geophys. Res.*, *116*.
- World Health Organization (2013), Health effects of particulate matter, policy implications for countries in eastern Europe, Caucasus, and central Asia.

FIGURES

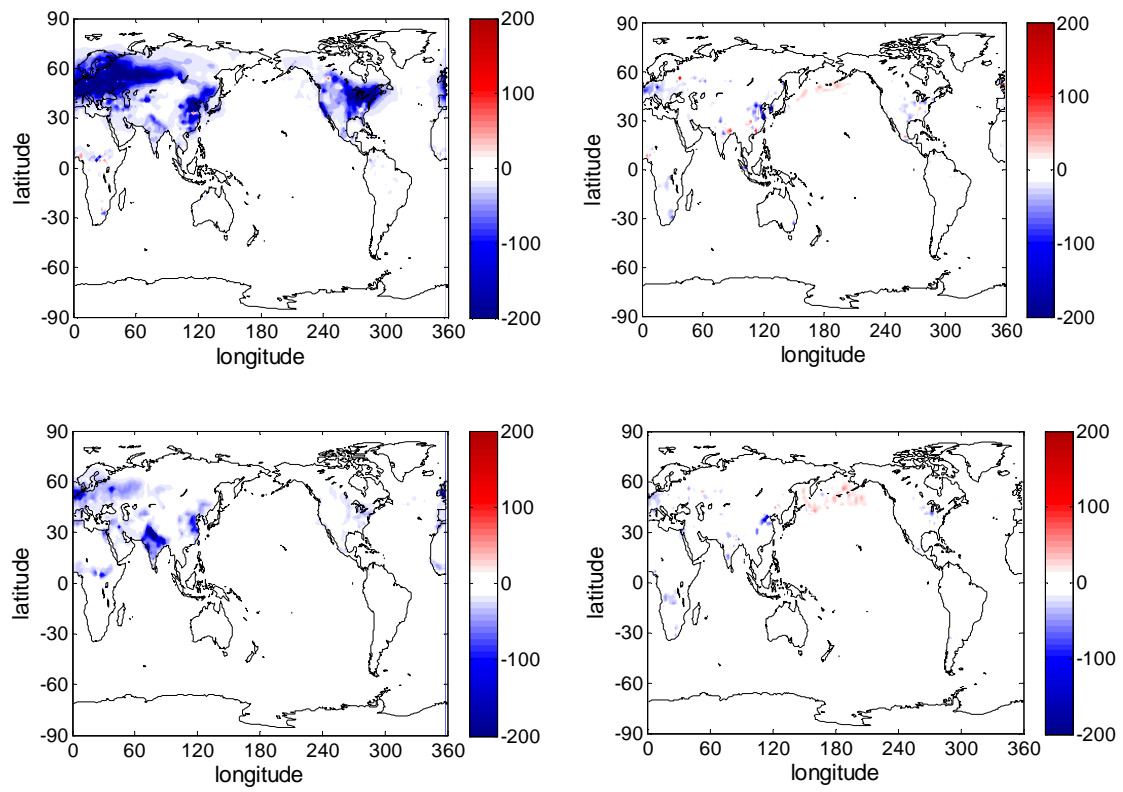


Figure 1. Surface NO_x aviation-induced perturbations (ppt) for January (left) and July (right). Present Day is on the top panel while Mid-Century SC1 is on the bottom.

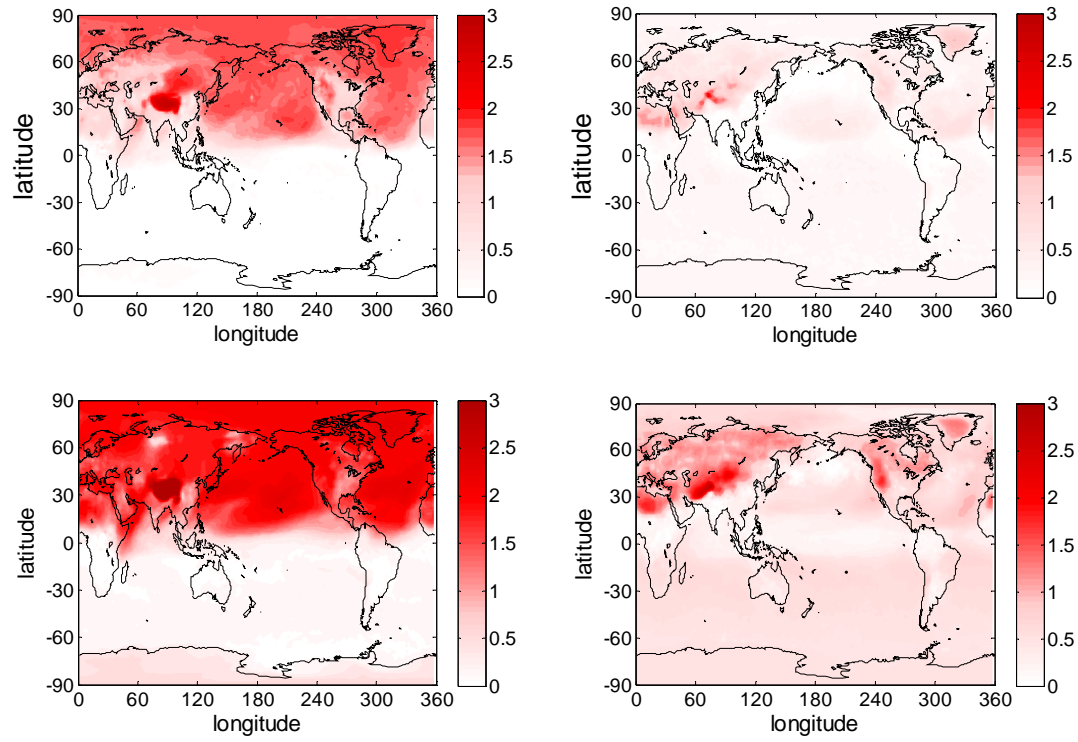


Figure 2. As in Fig. 1, but for O₃ (ppb)

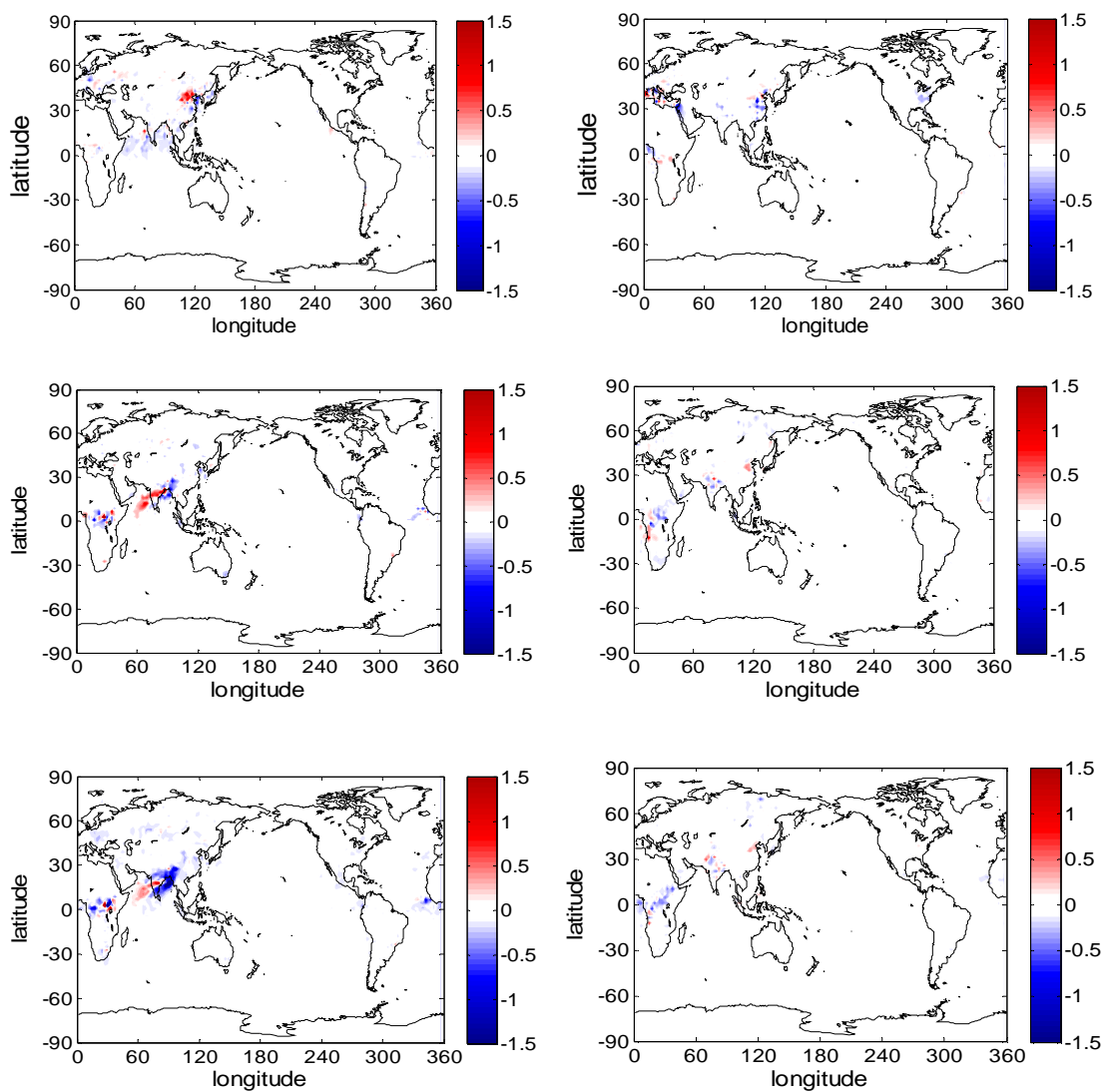


Figure 3. As in Fig. 1, but for PM_{2.5} ($\mu\text{g}/\text{m}^3$). The top panel is for Present Day, while the middle and bottom panels show Mid-Century SC1 and Alt, respectively

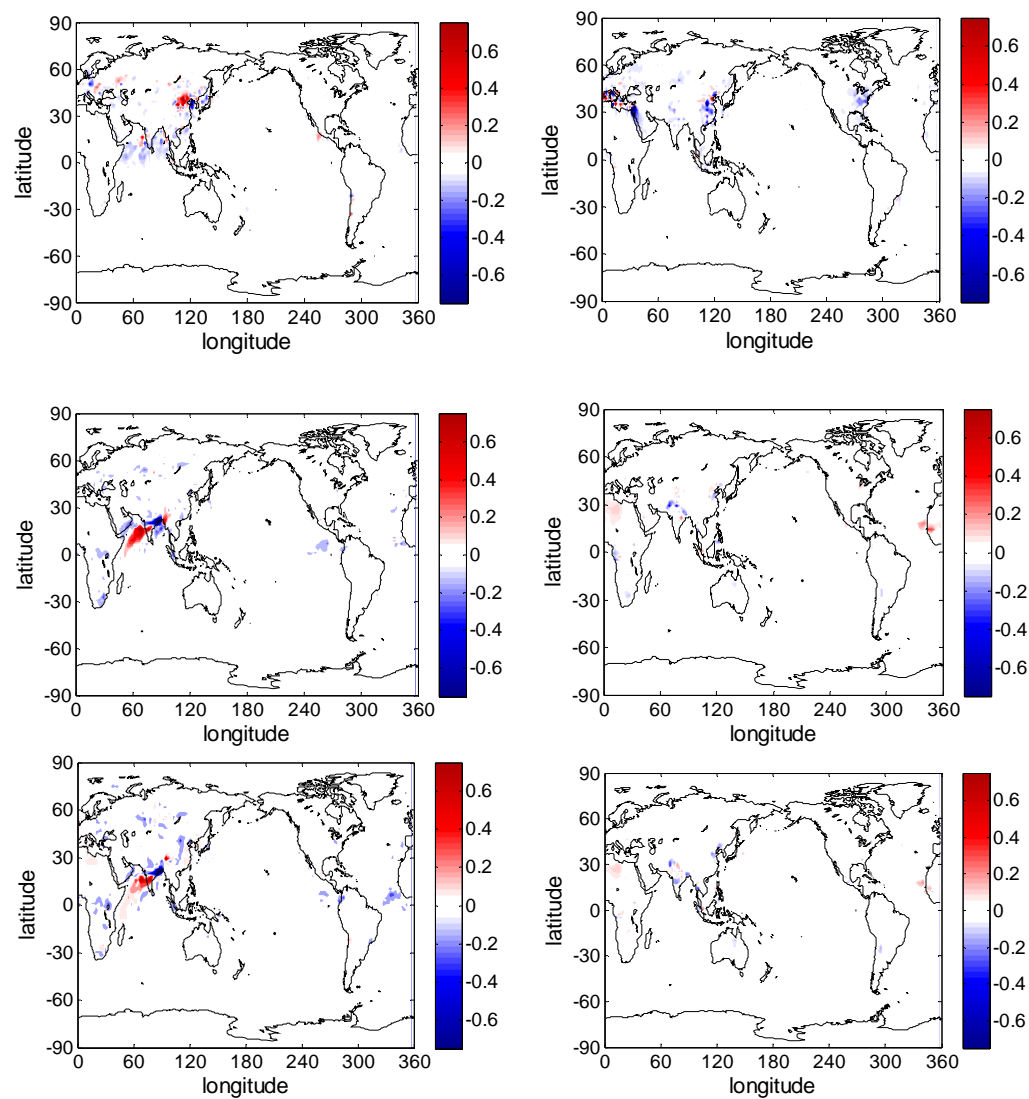


Figure 4. As in Fig. 3, but for SO_4^{2-} ($\mu\text{g}/\text{m}^3$).

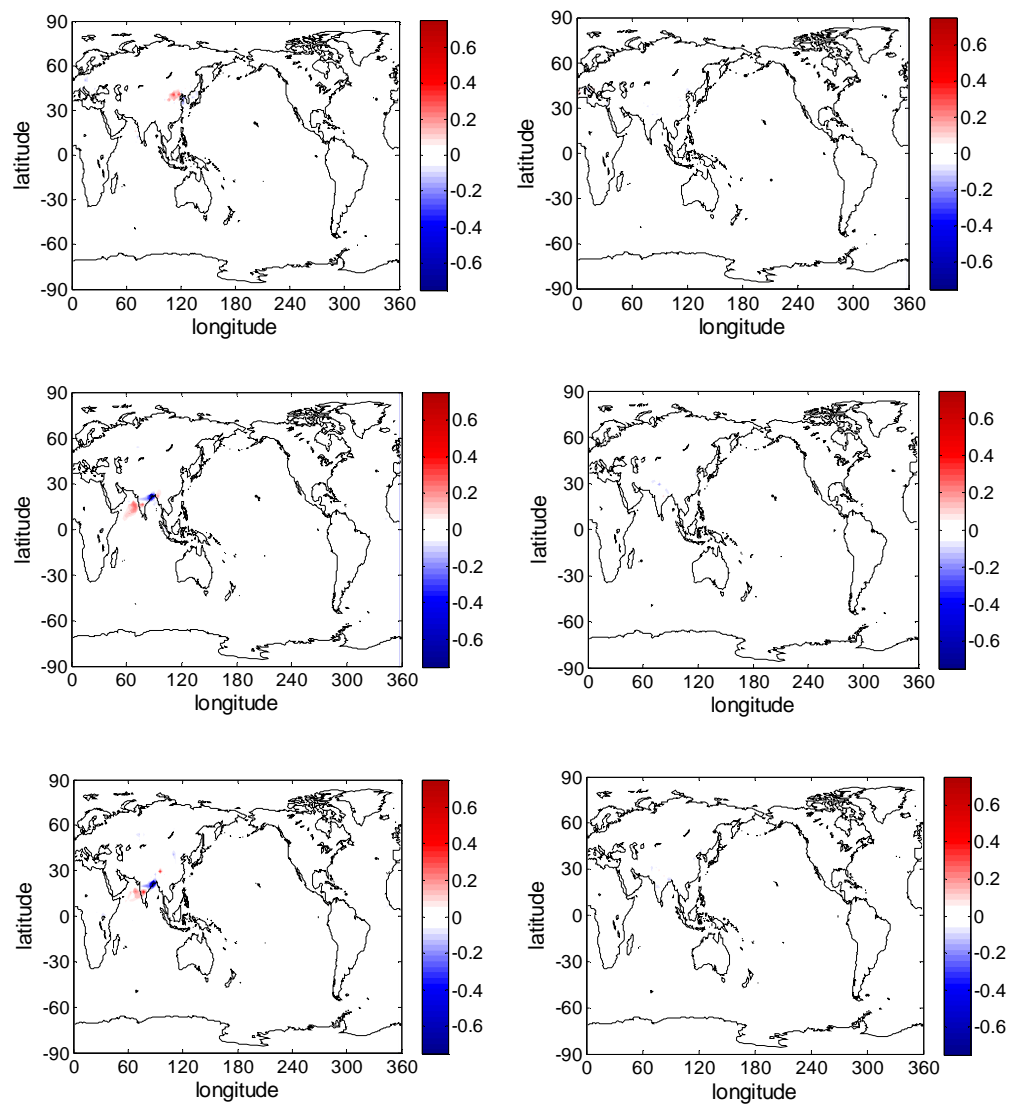


Figure 5. As in Fig. 4, but for NH_4NO_3 ($\mu\text{g}/\text{m}^3$).

TABLES

Table 1. Comparison of Emissions Scenarios. Only aviation emissions above 1 km (non-LTO) were used. ‘PD’ refers to present day while ‘SC1’ and ‘Alt’ are the two mid-century fuel scenarios.

| | NO_x(Tg N) | BC (Gg) | OC (Gg) | CO (Tg) | H₂O (Tg) | SO₂ (Tg) | SO₄ (Gg) |
|-----|-----------------------------|----------------|----------------|----------------|----------------------------|----------------------------|----------------------------|
| PD | 0.73 | 5.0 | 5.0 | 0.68 | 232.0 | 0.221 | 6.77 |
| SC1 | 1.38 | 13.7 | 11.0 | 0.86 | 559.8 | 0.53 | 16.74 |
| Alt | 1.38 | 6.9 | 11.0 | 0.86 | 559.8 | 0 | 0 |

Table 2. Present day (2006) and mid-century scenario 1 (2050) maximum 8-hour aviation-induced O₃ perturbations, mean background O₃ concentration, and maximum percent increases relative to background O₃ concentrations for January in four ‘hotspot’ regions, the Eastern USA (105 – 60° W, 30 – 50° N), Western USA (125 – 105° W, 30 – 50° N), Europe (15° W – 45° E, 35 – 65° N), and Southeast Asia (100 – 150° E, 20 – 45° N).

| O ₃ [ppb] 2006 | East USA | | West USA | | Europe | | S.E. Asia | |
|---------------------------|----------|------|----------|------|--------|------|-----------|------|
| | Jan | Jul | Jan | Jul | Jan | Jul | Jan | Jul |
| Max pert | 1.7 | 0.8 | 1.7 | 1.1 | 1.7 | 1.1 | 2.6 | 1.2 |
| Mean bg | 39.0 | 51.7 | 44.0 | 52.0 | 34.5 | 57.4 | 50.0 | 41.4 |
| % Perturbation | 4.4% | 1.5% | 3.8% | 2.1% | 4.9% | 1.9% | 5.2% | 2.9% |

| O ₃ [ppb] 2050 | East USA | | West USA | | Europe | | E. Asia | |
|---------------------------|----------|------|----------|------|--------|------|---------|------|
| | Jan | Jul | Jan | Jul | Jan | Jul | Jan | Jul |
| Max pert | 2.4 | 1.3 | 2.2 | 1.9 | 2.2 | 1.6 | 4.7 | 1.9 |
| Mean bg | 43.4 | 45.5 | 48.1 | 49.3 | 42.7 | 58.2 | 47.3 | 34.7 |
| % Perturbation | 5.5% | 2.9% | 4.6% | 3.9% | 5.2% | 2.7% | 9.9% | 5.5% |

Table 3. Frequency of grid points that exceed the EPA NAAQS standard due to aviation emissions for present day and mid-century (scenario 1) 8-hour maximum O₃ concentrations in three regions, the contiguous USA (125 – 60° W, 30 – 50° N), Europe (15° W – 45° E, 35 – 65° N), and Southeast Asia (100 – 150° E, 20 – 45° N)

| O ₃ (ppb) July | USA (300 grid pts x 31 days) | | Europe (400 grid pts x 31 days) | | SE Asia (294 grid pts x 31 days) | |
|--|---------------------------------|-------|------------------------------------|-------|-------------------------------------|-------|
| | 2006 | 2050 | 2006 | 2050 | 2006 | 2050 |
| Number of grids experiencing AQ events due to aviation emissions | 60 | 38 | 129 | 275 | 49 | 52 |
| Total number of grids | 9300 | 9300 | 12121 | 12121 | 9114 | 9114 |
| % increase | 0.65% | 0.41% | 1.06% | 1.44% | 0.54% | 0.57% |

Table 4. As in Table 3, but for PM_{2.5}.

| PM _{2.5} (µg/m ³) July | USA (300 grid pts x 31 days) | | Europe (400 grid pts x 31 days) | | SE Asia (294 grid pts x 31 days) | |
|--|---------------------------------|------|------------------------------------|-------|-------------------------------------|------|
| | 2006 | 2050 | 2006 | 2050 | 2006 | 2050 |
| Number of grids experiencing AQ events due to aviation emissions | 0 | 0 | 1 | 0 | 10 | 0 |
| Total number of grids | 9300 | 9300 | 12121 | 12121 | 9114 | 9114 |
| % increase | 0% | 0% | 0.01% | 0% | 0.11% | 0% |

Technical Report Documentation Page

| | | | |
|--|--|---------------------------------------|-----------|
| 1. Report No. | 2. Government Accession No. | 3. Recipient's Catalog No. | |
| 4. Title and Subtitle | | 5. Report Date | |
| | | 6. Performing Organization Code | |
| 7. Author(s) | | 8. Performing Organization Report No. | |
| 9. Performing Organization Name and Address | | 10. Work Unit No. (TRAIS) | |
| | | 11. Contract or Grant No. | |
| 12. Sponsoring Agency Name and Address | | 13. Type of Report and Period Covered | |
| | | 14. Sponsoring Agency Code | |
| 15. Supplementary Notes | | | |
| 16. Abstract | | | |
| 17. Key Words | | 18. Distribution Statement | |
| 19. Security Classif. (of this report) Unclassified | 20. Security Classif. (of this page) Unclassified | 21. No. of Pages | 22. Price |